Microelectronic Engineering 141 (2015) 267–279

Contents lists available at ScienceDirect

Microelectronic Engineering

journal homepage: www.elsevier.com/locate/mee

Review Article

Solid on liquid deposition, a review of technological solutions

Alexandra Homsy [a], Edith Laux [a], Laure Jeandupeux [a], Jerome Charmet [b], Roland Bitterli [c], Chiara Botta [d], Yves Rebetez [a], Oksana Banakh [a], H. Keppner [a,*]

[a] Haute Ecole Arc Ingénierie, HES-SO//University of Applied Sciences Western Switzerland, Eplatures-Grise 17, CH-2300 La Chaux-de-Fonds, Switzerland
[b] Nanoscience Centre Department of Engineering University of Cambridge, 11 J.J. Thomson Avenue, Madingley Road, Cambridge CB3 0FF, UK
[c] Ecole polytechnique fédérale de Lausanne (EPFL), Institute of Microengineering, Instant Laboratory, Rue de la Maladière 71B, 2000 Neuchâtel, Switzerland
[d] Istituto per lo Studio delle Macromolecole, CNR Via Bassini 15, 20133 Milano, Italy

ARTICLE INFO

Article history:
Received 7 November 2014
Received in revised form 24 March 2015
Accepted 25 March 2015
Available online 8 April 2015

Keywords:
Thin solid films
Solid on liquid
Nucleation
MEMS
Parylene
Solid on liquid deposition

ABSTRACT

Solid-on-liquid deposition (SOLID) techniques are of great interest to the MEMS and NEMS (Micro- and Nano Electro Mechanical Systems) community because of potential applications in biomedical engineering, on-chip liquid trapping, tunable micro-lenses, and replacements of gate oxides. However, depositing solids on liquid with subsequent hermetic sealing is difficult because liquids tend to have a lower density than solids. Furthermore, current systems seen in nature lack thermal, mechanical or chemical stability. Therefore, it is not surprising that liquids are not ubiquitous as functional layers in MEMS and NEMS. However, SOLID techniques have the potential to be harnessed and controlled for such systems because the gravitational force is negligible compared to surface tension, and therefore, the solid molecular precursors that typically condense on a liquid surface will not sediment into the fluid. In this review we summarize recent research into SOLID, where nucleation and subsequent cross-linking of solid precursors results in thin film growth on a liquid substrate. We describe a large variety of thin film deposition techniques such as thermal evaporation, sputtering, plasma enhanced chemical vapor deposition used to coat liquid substrates. Surprisingly, all attempts at deposition to date have been successful and a stable solid layer on a liquid can always be detected. However, all layers grown by non-equilibrium deposition processes showed a strong presence of wrinkles, presumably due to residual stress. In fact, the only example where no stress was observed is the deposition of parylene layers (poly-para-xylylene, PPX). Using all the experimental data analyzed to date we have been able to propose a simple model that predicts that the surface property of liquids at molecular level is influenced by cohesion forces between the liquid molecules. Finally, we conclude that the condensation of precursors from the gas phase is rather the rule and not the exception for SOLID techniques.

1. Introduction

Solid-on liquid deposition (SOLID) techniques for applications in the MEMS/NEMS field are generally defined as techniques where solid films coat a previously patterned liquid (e.g. in the form of drop arrays or thin liquid films) onto a solid substrate. Note that in general this solid film is deposited so that there are no bubbles within the liquid, and we are only dealing with *films* in this review, not the case of simply putting fluid into a container and sealing it with a solid cap.

The functionalities of SOLID techniques can be classified into the following:

(i) Sustainable systems where perfect encapsulation of liquids could have an impact on the optical or the mechanical properties (e.g. intraocular lenses).
(ii) Drug delivery systems where the solid membrane releases the encapsulated liquid on demand.
(iii) Liquid functional layers for MEMS (e.g. liquid waveguides, microfluidic systems, liquid computing).
(iv) MEMS/NEMS construction concepts using sacrificial liquid volumes (e.g. free standing membranes, cantilevers, flap-valves).

SOLID is not straightforward since the density of the solid tends to be higher than the liquid; hence due to Archimedes' principle, macroscopic assemblies resulting from condensation of the vapor

* Corresponding author. Tel.: +41 765571364.
E-mail addresses: alexandra.homsy@he-arc.ch (A. Homsy), edith.laux@he-arc.ch (E. Laux), laure.jeandupeux@he-arc.ch (L. Jeandupeux), jc715@cam.ac.uk (J. Charmet), roland.bitterli@epfl.ch (R. Bitterli), c.botta@ismac.cnr.it (C. Botta), yves.rebetez@he-arc.ch (Y. Rebetez), oksana.banakh@he-arc.ch (O. Banakh), herbert.keppner@he-arc.ch (H. Keppner).

http://dx.doi.org/10.1016/j.mee.2015.03.068
0167-9317/

Table 1
Fabrication methods and examples of solid on liquid deposition (SOLID) systems.

Method	Description	Example	Illustration
Vapor phase methods Without reaction See Section 3	Atoms or molecules are released from a solid or liquid into the vacuum. They condense as solid material on a liquid surface	Thermal deposition of poly-para-xylylene (PPX), condensation and crosslinking on liquids Evaporation of Au or Al Sputtering of Au, Ti or Al Decomposition of SiH_4, CH_4, into reactive species that condense on a liquid	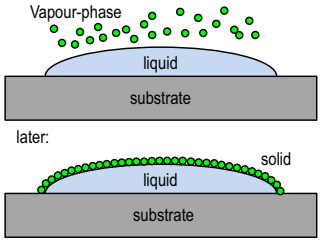
Vapor phase methods With reaction See Section 4	From a solid or liquid source an atomic or molecular vapor is released into vacuum that reacts chemically with the molecules of a liquid at condensation, thus forming a solid layer. This reaction can also be plasma induced	Unsaturated fluorenes reacts with PPX at condensation	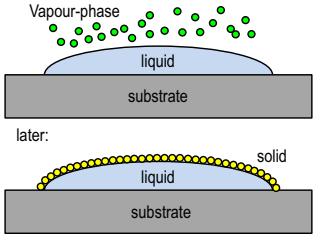
Liquid phase methods Without reaction See Section 5.1	Two non miscible liquids; if the low-density liquid (on top) can result in a sol–gel deposition, the underneath high density liquid becomes encapsulated	Low-density sol–gel liquid: TEOS $Si(C_2H_5O)_4$; High-density "bottom" liquid: ionic liquid such as 1-butyl-3-methylimidazolium-tetrafluoroborate (BMIM)	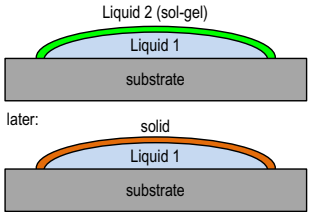
Liquid phase methods Without reaction See Section 5.2	Two non-miscible liquids; the high-density "bottom" liquid is inert, the top-liquid is a dissolved polymer. At evaporation of the solvent, the polymer crosslinks to become a solid layer	Ter-fluoro polymer THV-220 in acetone on glycerol	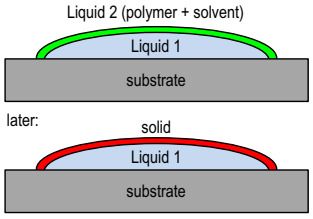
Liquid phase methods With reaction (sonochemistry) See Section 5.3	An emulsion in water together with a protein phase. At ultrasound energy, water is converted into H_2O_2 that gives rise to denaturation and subsequent crosslinking of the protein. Shells are created around the emulsion	Emulsion: tetracycline (TTCL) droplets; Protein: BSA in water	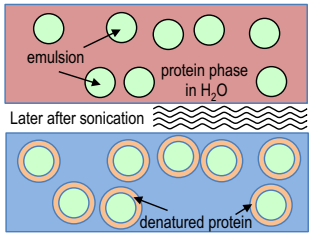

phase risk sedimenting to the bottom of the liquid. However, we know that gravitation forces are completely negligible compared to the inter-molecular forces keeping the molecules of the liquid together at the nanoscale. In other words, it should be potentially possible to coat *any* liquid surface with *any* solid if the length scale is on the appropriate order. Table 1 summarizes existing methods and examples of SOLID solutions using these principles.

In this review, we first identify SOLID systems that can be found in nature, daily life or in the laboratory. Then we present each of the examples identified in Table 1, with an emphasis on their fabrication method and potential impact for applications.

2. Observation of solid on liquid deposition in nature, daily life and in the laboratory

Several well-known examples of SOLID can be observed in nature, in our daily life, or in the laboratory; they are all macroscopic examples and represented in Fig. 1.

In Fig. 1a, plants have settled down on a lake giving the impression of a solid surface. Upon close examination, however, we note that the plants do not hermetically cover the water. In Fig. 1b, a solid layer of sulfur can be observed on top of a hot source of liquid due to bacterial activity. Fig. 1c shows blood in various states; blood coagulates as soon as it comes in contact with oxygen, forming a solid material that heals the injury. Fig. 1d shows protein denaturation in milk due to heating above 60 °C resulting in solidification of the surface. In Fig. 1e, a water drop is poured onto an old sulfur containing cast iron disk; after several hours, a thin iron/sulfur oxide layer covers the drop, showing interference colors. Fig. 1f shows ice on water. The density of water is greatest at 4 °C hence ice has a lower density than water. As a consequence, lakes freeze at the surface. In Fig. 1g, a skin can be observed on the surface of forgotten tea after cooling down due to solidification of impurities in the water. Fig. 1h shows partly dried paint spluttered on the lid of its can; polymerization or

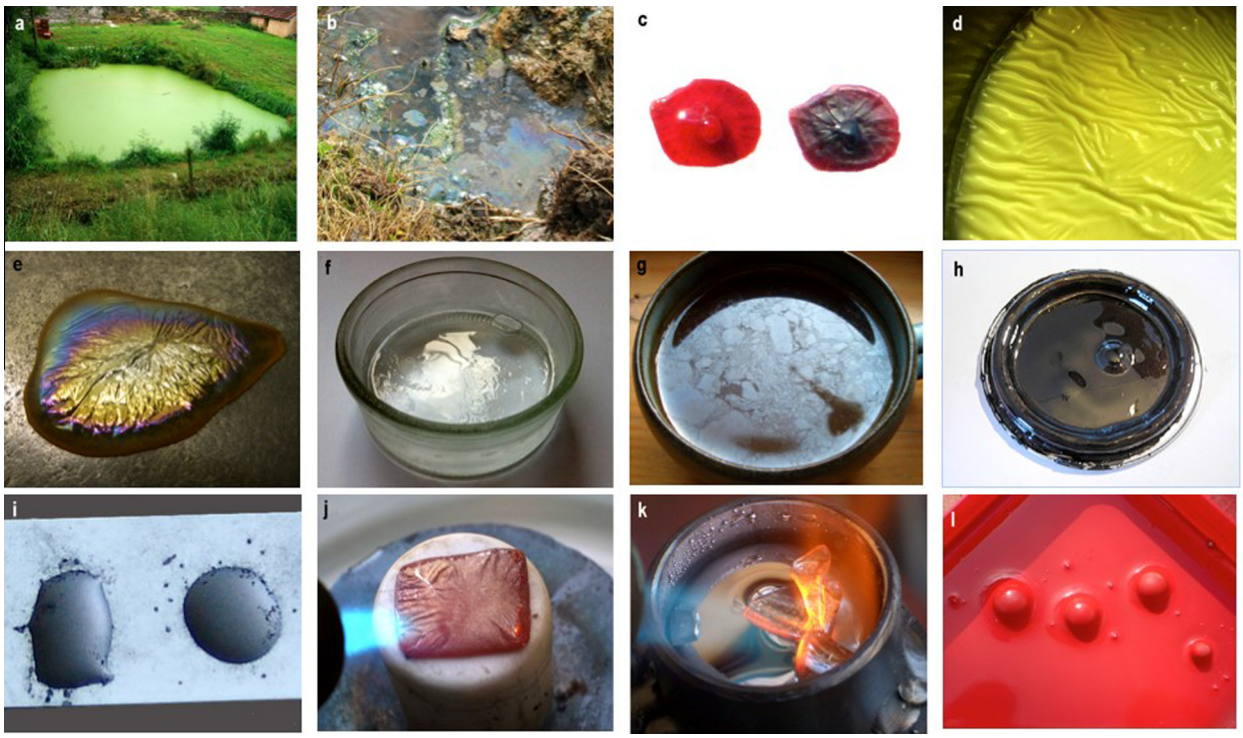

Fig. 1. (a–d) Shows SOLID examples observed in nature: (a) a lake covered by plants; (b) sulfur released for bacterial activity; (c) fresh and partially agglomerated blood; (d) skin on hot milk; (e and f) shows examples that can be observed in daily life: (e) is a thin Fe/S/O_x layer on water; (f) ice on water; (g) a skin on cold tea; (h) partially dried paint on a lid; (i–l) are examples obtained by technical effort: (i) fine graphite powder aligned on a water surface; (j) shows solid Al_2O_3 on liquid aluminum; (k) solid float-glass on liquid tin; (l) dried paint sprayed on mercury.

desiccation of the liquid occurs due to evaporation of the solvent, and after a while, the whole droplet becomes solid. If small particles such as graphite powder are spread on a droplet of water, they self-align, resulting in a solid surface as represented in Fig. 1i. Alumina on hot aluminum (Al) is shown in Fig. 1j. If solid Al is heated, it will become liquid at 660 °C. Due to the presence of oxygen, Al is oxidized. Aluminum oxide has a melting point of more than 2000 °C and hence will cover the liquid Al with a stable solid layer as long as the temperature is above the melting point of Al. Note that the lattice constant of Al_2O_3 needs more surface than the liquid Al surface can offer, hence wrinkles are formed. Fig. 1k shows the well-established technique of float-glass fabrication. In this process, liquid glass is cast onto liquid tin at high temperature; it "floats" at the surface of the tin-bath due to its lower density. The liquid phases are not miscible and the liquid tin shapes the bottom surface of the glass allowing for the glass surface roughness to be minimized. The last example, Fig. 1l, shows dried sprayed paint on liquid mercury. One more thing to note about this array of pictures is the length scale. For example, the solid layer represented in Fig. 1a is at meter scale. All other layers show rather thin layers (micrometer thickness) but their lateral extension are at macroscopic centimeter scale. It may be assumed that if the solid layer were molecular, liquids quantities in the microliter range could be totally encapsulated.

In addition to not being completely encapsulated in all cases, these examples of SOLID systems also lack thermal, chemical or mechanical stability. There is little chance for importing such natural inspired SOLID systems for device purposes as summarized above in Section 1i–iv. On the contrary, the different technologies presented in the following sections will have the potential in stable solid on liquid coatings.

3. Vapor phase methods

3.1. Solid on liquid by CVD

3.1.1. LPCVD PPX-based solid on liquid deposition

The first promising solution to obtain SOLID structures was pioneered by the authors in previous work [1,2] and confirmed by [3]. In this work, the polymer poly-di-chloro-para-xylilene (PPX-C), also known as parylene C, was grown on low vapor pressure liquids (up to 5 Pa pressure) using a conventional PPX LPCVD process also known as the Gorham process [4]. This process is summarized as follows. Parylene C is deposited by a LPCVD reactor where the precursor (the dimer dichloro[2,2]-paracyclophane) is released from the solid phase to vapor by sublimation at typically 150 °C and vapor pressure of 5 Pa. In a downstream set-up (Fig. 2a and b), the dimer is cracked by thermal pyrolysis at 650 °C. During this process, the resulting radical polymerizes in a chain-growth of PPX (Fig. 2b). On its way to the deposition chamber (kept at room temperature), the monomer converts from the highly reactive triplet state (benzoid, paramagnetic di-radical) to the less reactive singlet state (quinonoid, diamagnetic) according to [5]. Thermodynamic dimer to monomer conversion and deposition kinetics is reviewed in detail in [5]. The monomer in the singlet state is, according to [6], physisorbed with no activation energy and has low sticking coefficient and a high surface mobility. This fact explains the high conformity of parylene-coated surfaces. Polymerization is initiated by dimerization of two monomers leading to a biradical dimer. The chain propagation is enabled by attachment of a monomer to the radical chain end [6]. This perfect coverage of surfaces of the resulting polymer was demonstrated at the molecular scale [7].

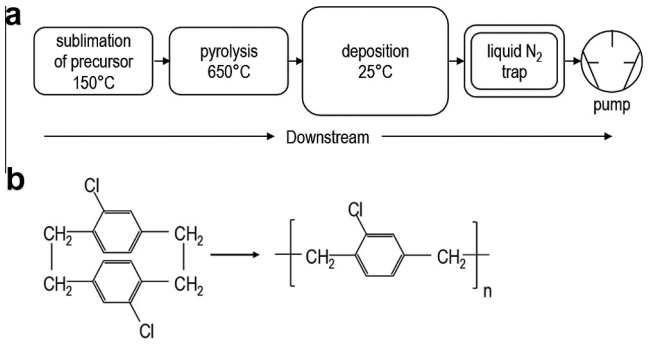

Fig. 2. (a) sketch of a LPCVD parylene C (PPX-C) deposition reactor according to [4]. (b) PPX-C precursor and polymerization.

When depositing parylene on a low vapor pressure liquid, a polymer layer is growing over the liquid. Typical liquids for creating such SOLID structures have a vapor-pressure at least one order of magnitude less than the process pressure (5 Pa). Liquids such as glycerol or bis-(3,5,5-trimethylhexyl) phthalate allow the replication of typical liquid-driven shapes that are strongly defined by contact angle effects. The perfect replication of a liquid surface was verified by measuring the contact angle before and after PPX-C deposition [2] (see Fig. 3a), where it was shown that the shape of the drop was not affected by the thickness of the PPX layer up to 5.5 μm. It is expected that increasing the PPX thickness even up to 100 μm will not induce a change in the contact angle. This effect is not limited to PPX on the (bis-(3,5,5-trimethylhexyl)) phthalate liquid, but works also for a large variety of other liquids (e.g. 1,2-cyclohexanedicarboxylic acid di-isononyl ester, bis(2-ethylhexyl) adipate, different oils, silicone oils, glycerol etc.).

By peeling-off and cleaning the PPX-C layer deposited on silicon oil, the roughness of the PPX-C in contact with the oil was measured to be about 1 nm using AFM techniques [2] (see Fig. 3b). Assuming that the liquid is smooth at molecular level, the results let conclude that the PPX-C growth comes close to replicating the liquid's surface. In fact, with glycerol and most oils, the surface roughness of both the top and bottom of the PPX-C is extremely small (1 nm or less). However, a pronounced porosity of the film has been found [8] for some liquids like e.g. 1,3,5-trimethyl-1,1,3,5,5-pentaphenyl-trisiloxane (HIVAC-F5).

3.1.2. Applications of LPCVD PPX-based solid on liquid deposition

The most obvious applications using this fabrication method are liquid lenses due to the outstanding optical quality at the liquid surface (smoothness at molecular level due to surface-energy minimization). Fig. 4 shows conformal PPX packaging of such lenses.

Apart from lens structures shown in Fig. 4 more complex 3 D structures could be prepared. In this case self-assembled monolayers (SAMs) as good chemical traps were patterned by photolithography using the molecular-assembly patterning by lift-off (MAPL) process [9]. Fig. 5a–c shows that liquid feature sizes of several micrometers can be encapsulated.

Fig. 5d is similar as Fig. 4a where the shape of the drop is driven only by physico-chemical effects and not by trapping (where the contact angle depends on the quantity of liquid). Fig. 5d shows that very small droplets (<5 μm) can be coated. PPX on liquid represents a real packaging layer in a way that a solid interface is created allowing subsequent MEMS processing, such as metallization [3], patterning by photolithography, ion-beam implantation and structuration [10], or laser induced patterning

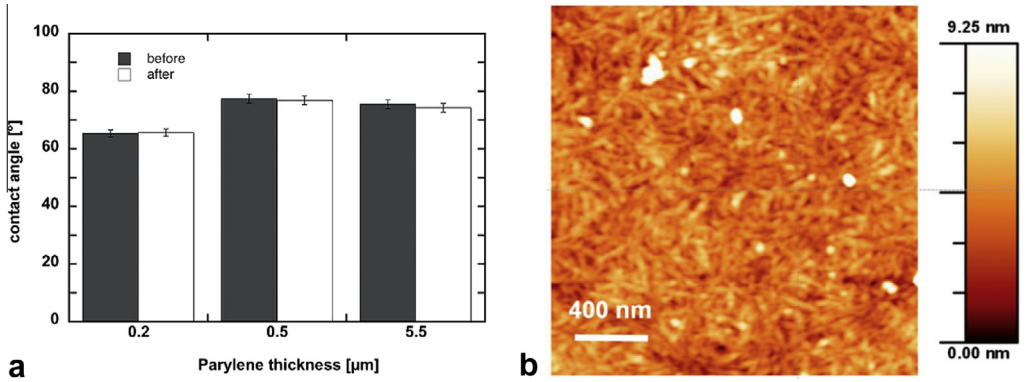

Fig. 3. (a) Contact angles of liquid drops of bis-(3,5,5-trimethylhexyl) phthalate on a substrate before and after PPX deposition [2, permission]. (b) AFM micrograph (2 × 2 μm) of the parylene interface grown directly on the liquid substrate and corresponding *z*-axis scale bar. The average RMS roughness is 1.28 ± 0.26 nm [2, permission].

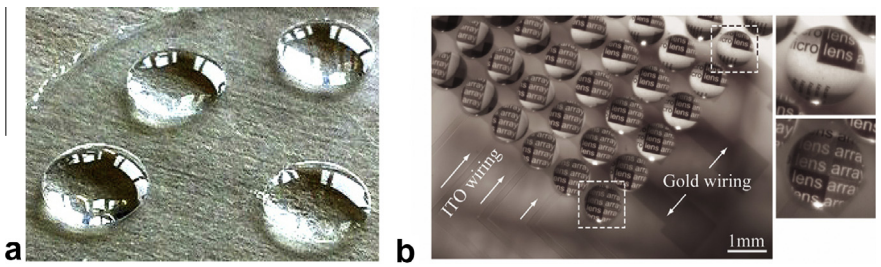

Fig. 4. (a) 2 μm thick PPX layer deposited on 2 mm diameter sized glycerol drops on a glass substrate. Each drop is forming a lens; in this case the shape of the lens is fully determined by the physico-chemical properties of the liquid, the interface, and the quantity of the liquid; the boundary seen on the left is the extremity of the glass substrate on which the drops were deposited; (b) micro lens array using 1–1.5 μm thick PPX on silicone oil on ITO coated glass substrate; on the PPX, a 5 nm Gold layer was deposited; in this case the shape of the lens is determined by chemical trapping due to the substrate properties [3, permission].

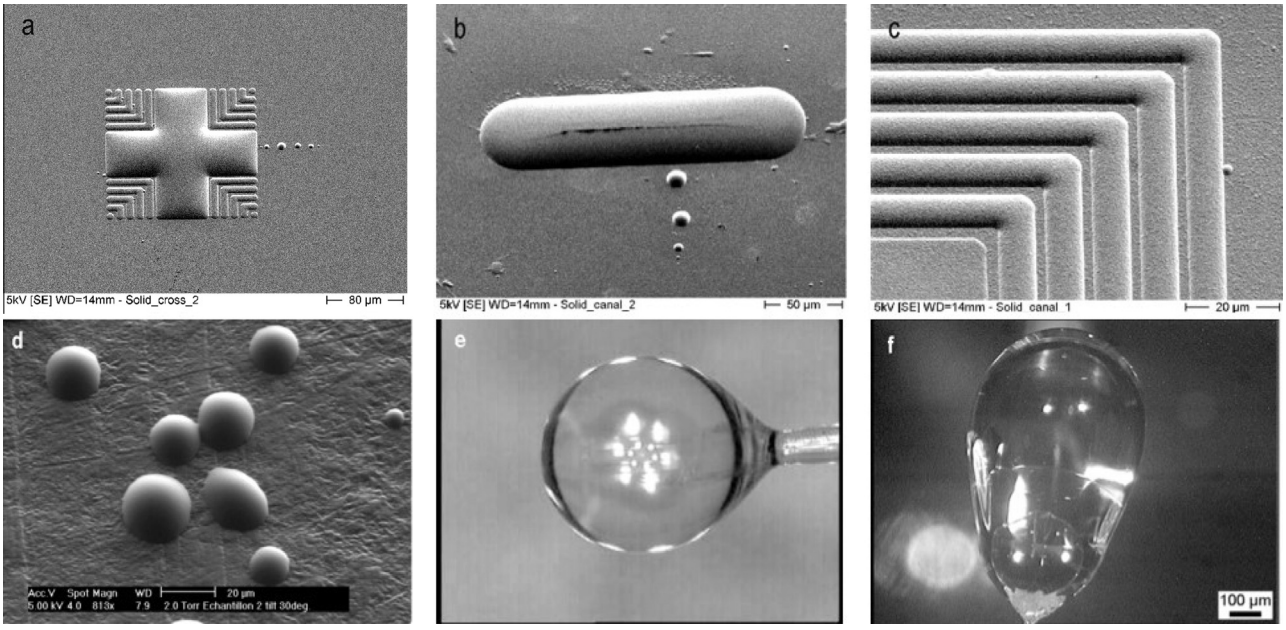

Fig. 5. (a) PPX-C encapsulation of glycerol that has been chemically trapped by a philic pattern on a phobic substrate; the patterning was done by photolithography; (b) and (c) channel-structures obtained in the same way as in (a); (d) silicon oil aerosol droplets coated with 5 µm thick PPX; (e) silicon oil drop at the end of an optical fiber, perfectly packaged with PPX; (f) polymer/liquid/polymer "onion" obtained by three successive dippings of an optical fiber into silicon oil, and PPX coatings. For all examples the PPX thickness was typically between 1 and 2 µm. The thickness of the gold sputtered layer for SEM measurements was 25 nm.

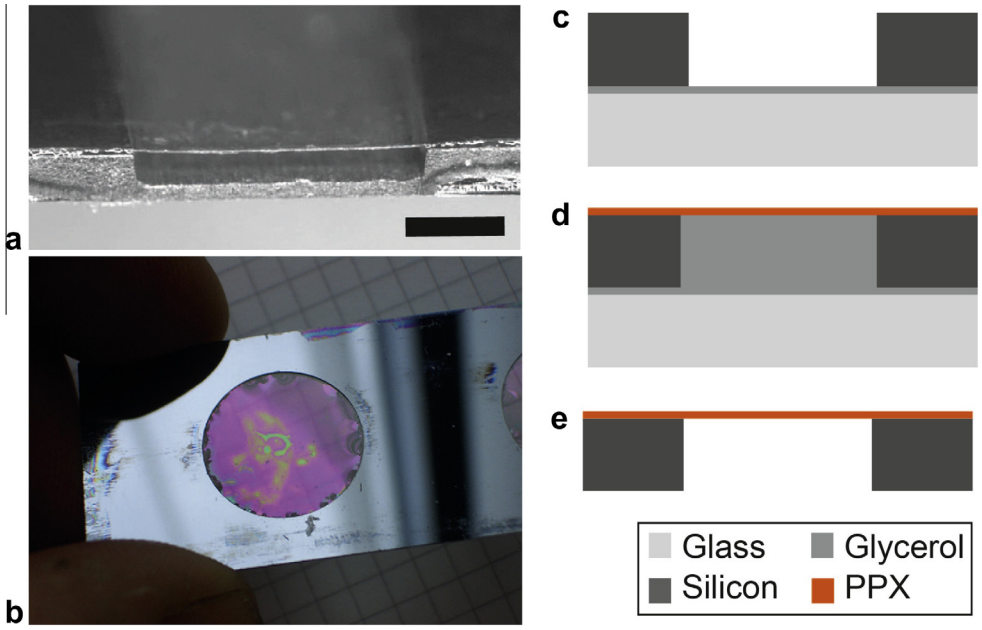

Fig. 6. (a) Cross-sectional view of a closed channel obtained by sacrificial liquid (glycerol in this case) removal after 5 µm PPX deposition on the liquid; the scale bar is 0.5 mm long; (b) large area (2 cm diameter) self-supporting 5 µm PPX layer after shearing off the bottom of a liquid containing well; (c–e) schematic explanation of the process steps driving to the result seen in (b): (c) a hole is drilled in a silicon substrate; this substrate is then put into contact with a glass substrate, hence forming a well; a thin layer of glycerol at the interface between substrates ensures good sealing; (d) the well is filled with glycerol, and a 5 µm PPX layer is coated by LPCVD; (e) after PPX deposition, the silicon is sheared off from the bottom glass substrate to release the liquid (glycerol) and hence revealing the PPX self-supporting membrane.

[11] as on any solid thin-film. Furthermore, PPX is a chemically stable, biocompatible, and mechanically resistant material [12]. Other 3 D structures that are defined by the properties of a liquid can hence be prepared. In Fig. 5e, a liquid drop at the end of an optical fiber can be packaged in PPX, in an another case the packaged drop was again dipped into the liquid and coated forming an "onion" type structure as shown in Fig. 5f.

Other examples of low vapor pressure liquids are e.g. liquid crystals, ferro fluids, oils, higher alcohols and ionic liquids (IOLs). Ionic liquids have interesting properties for thermoelectric generators. For this application hermetic packaging of the IOLs is essential; promising tests have been successfully carried out by [13–14].

If the PPX layer is opened and the liquid (glycerol) removed, a closed channel can be fabricated as shown in Fig. 6a. In this

example, a liquid was trapped in a laser micro-machined channel in a silicon substrate. Subsequent PPX deposition (5 μm) sealed the liquid hermetically. After PPX opening (e.g. laser drilling of liquid inlet and outlet) and removal of the liquid (by vacuum aspiration), the freestanding PPX coverage of the micro channel is obtained. Fig. 6b shows a large area self-supporting 5 μm thick PPX layer. This layer was obtained by shearing off the bottom of a liquid-filled well after PPX deposition. The well was drilled through a silicon wafer by femto-second laser machining, and put in contact with a glass substrate. A thin oil layer ensured hermetic sealing of both substrates during PPX deposition, but it also enabled the shearing off of both substrates after PPX deposition (see Fig. 6c–e for a schematic view of the process).

It can be imagined that, for any solid-on-liquid systems, the sacrificial liquid technique could be used for effective development of structures.

3.1.3. Atmospheric pressure CVD (APCVD) parylene-based solid on liquid

The common feature of the solid on liquid deposited systems of Sections 3.1.1 and 3.1.2 is that only low vapor-pressure liquids can be successfully encapsulated using PPX as promising packaging material. For applications such as drug delivery systems, it is imperative to be able to package aqueous liquids. However such liquids have a vapor pressure of about 2000 Pa at room temperature. This makes LPCVD deposition impossible, as it would lead to the evaporation of the aqueous droplets. To overcome such issues, we developed an atmospheric pressure CVD process for PPX deposition on aqueous liquids.

For this purpose the so-called Gorham process [4] was modified to work at pressures close to atmospheric pressure. Therefore the reactor has to be filled up with an inert gas (e.g. N_2 or Ar) up to atmospheric pressure. The inert gas was preferred with respect to air for avoiding chemical reactions of the dimer vapor with air. In this way the first SOLID structures on water could be deposited at a pressure of 80 kPa (Fig. 7). In contrast to the deposition scenario described in Fig. 2, the crucible for the APCVD process had to be heated up to about 220 °C instead of 150 °C to overcome the higher pressure in the reactor (atmospheric pressure instead of 1 Pa). Here the process parameters are more delicate to control due to the exponential increase of the vapor pressure as soon as the temperature of the sublimation source varies [15–16]. As seen in Fig. 7, the PPX surface is not perfect throughout the entire surface area and some wrinkles appear, probably due to liquid loss during coating.

3.2. Solid on liquid by physical vapor deposition (PVD)

The question arises looking at the large variety of inspirations given by natural SOLID systems (see Fig. 1) whether CVD PPX is the only material that can be deposited onto a liquid or not. The question is furthermore of scientific interest looking at the statement that at molecular level a liquid substrate appears as "hard" as a solid substrate, the forces from gravitation being neglected at this molecular scale. Therefore the authors, using e.g. silicon oil as low-vapor pressure liquid substrate, have carried out a large variety of deposition process and materials from the vapor phase. Table 2 gives the overview of the processes (left column) that deliver the vapor (right column); all experiments have been carried out on anhydrous silicon oil as substrate.

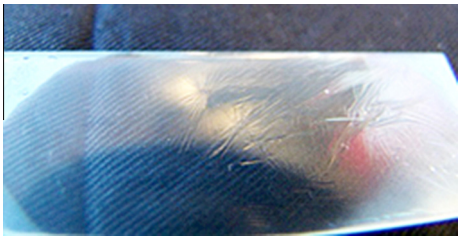

Fig. 7. PPX deposited on water on a glass substrate at a pressure of 80 kPa; a black tissue was put underneath for better contrast. The water is spread over the entire substrate of a 76 × 26 mm glass substrate. Possibly a small water loss occurred during deposition; this could explain the appearance of small wrinkles.

The SOLID layers obtained from the experimental conditions presented in Table 2 are depicted in Figs. 8–10 where typical PVD systems have been used without any optimization of the deposition processes. The silicon oil has a low vapor pressure ($<10^{-4}$ Pa), and it was assumed that no molecules were released from the liquid at the pressure that was applied for the coating. The observation and the statements are based on visual inspection of the results using a microscope.

Further test have been carried out using atmospheric plasma CVD depositions; the cold plasma corona discharge of strongly diluted silane-gas 0.5% SiH_4 in Argon gas mixture was powered by a downstream tesla coil at 13.56 MHz; the set-up is shown in Fig. 11a, and the deposition on silicon oil is shown in Fig. 11b. In a second series of experiments, a silent discharge downstream configuration was setup for depositing Teflon-like polymers on liquid (see Fig. 12) using a CF_4–Ar mixture (5%). The results show very thin (Fig. 12b) and very thick (Fig. 12c) layers without wrinkles, like the PPX layers coated by CVD. We assume that, due to the downstream property of the coating technique, the ion bombardment-induced stress on the SOLID layer is strongly reduced, and hence very few wrinkles were created. Further systematic studies (at low and atmospheric pressures) must be carried-out on stress release effects.

In summary, looking at this large variety of deposition methods from the vapor phase, all resulted in the deposition of thin solid films on a liquid substrate. However, all layers exhibited strong deformation and wrinkle formation after the nucleation due to internal stress. Apart from Teflon-like coatings at atmospheric pressure, the previously discussed PPX deposition (Section 3.1) seems to be the exception where perfect replication of the liquid substrate can be obtained. The simple sketch model on Fig. 13 takes a closer look at the molecules covering the liquid phase after the very first nucleation of a thin-film on the substrate and gives an explanation as to why the strong wrinkles do appear after that. This Fig. 13 shows particles (molecules, atoms), which are arriving from the vapor phase to the surface of the liquid and attach to it by weak bonds. Further increase of the particle density let cross-link the particles by bond strengths that are typical for thin films. The residual force that brings the energy of the thin film to a minimum will be the one to determine the shape of the thin film. The liquid surface will no more determine the shape of the thin film. The more the thickness of the thin film, the more internal stress (tensile or compressive) will dominate shaping of the whole SOLID system. This is why wrinkles appear. This effect is also observed for most of the vapor phase deposition processes. A sputtered thin-film layer (e.g. Al, Ti, etc.) that is deposited onto a glass substrate peels off as soon as the layer thickness exceeds 4 μm because the

Table 2
Summary of the PVD processes and vapor materials, which have been deposited by the authors on anhydrous silicon oil drops on glass substrates.

Deposition process	Vapor
Thermal evaporation in high vacuum	Aluminum
Sputtering at 0.5 Pa	Gold
PECVD at 50 Pa	CF_4–Ar, SiH_4
Atmospheric PECVD	HMDS, SiH_4, C_2H_4

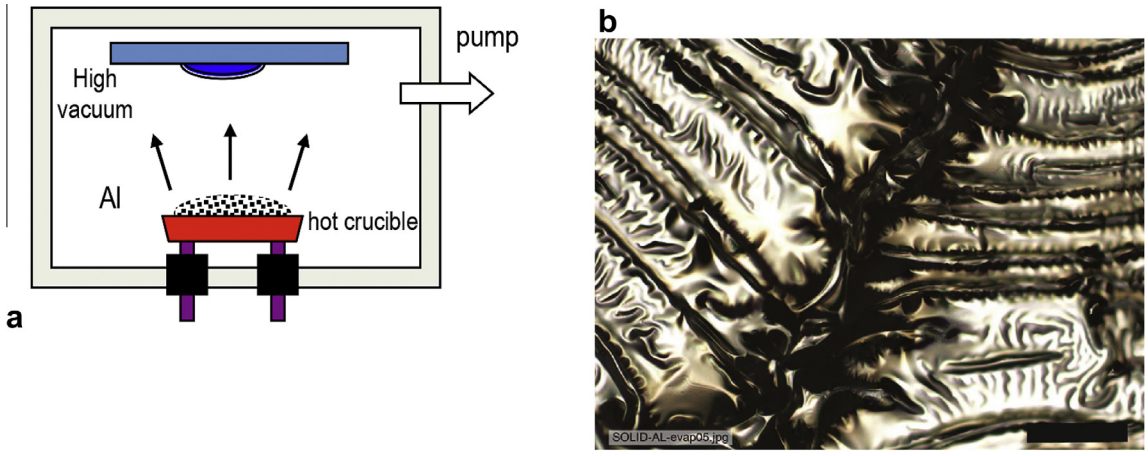

Fig. 8. (a) Sketch of the experimental layout for thermal evaporation of aluminum on silicon oil. (b) 200 nm thick aluminum thin-film on liquid silicon oil. The scale bar is 100 μm long.

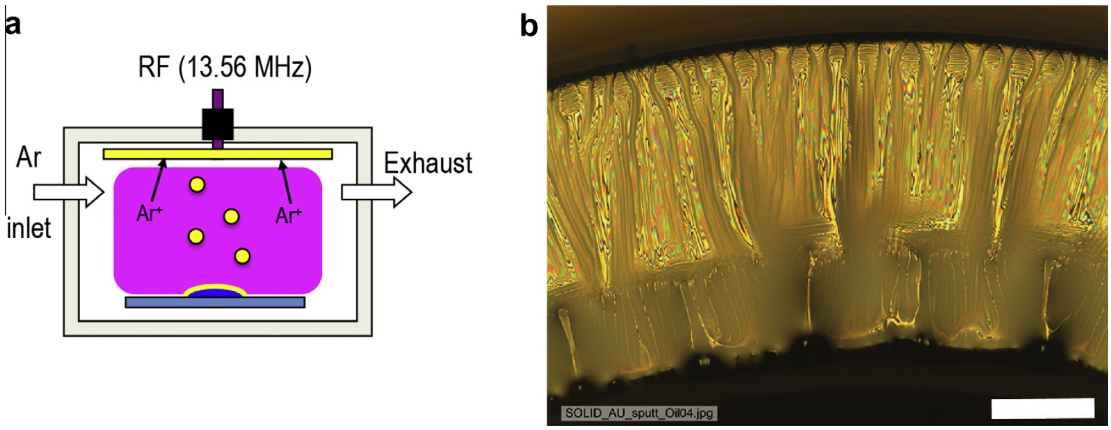

Fig. 9. (a) Sketch of the experimental layout for sputtering of gold on silicon oil. (b) A sputtered 200 nm thick gold thin film on silicon oil. The scale bar is 200 μm long.

accumulated internal stress creates a strain that is larger than the bond strength per unit area. It appears that PPX is the only solid-state material (to the knowledge of the authors) that is not deforming its nucleation plane even up to 100 μm thickness.

4. Vapor phase methods with surface reaction

4.1. LPCVD PPX deposition with surface reaction

In the previous observation it was assumed that the liquid is chemically passive looking at nucleation between the precursors of the PPX monomers. In this section, the PPX layer is still coated with the same LPCVD technique, but the liquid on which the PPX is coated will react with the PPX precursors. For liquids that have a low vapor pressure such as glycerol, (bis-(3,5,5-trimethylhexyl)) phthalate, or oils, the conventional Gorham process [4] was tested. For high vapor pressure liquids the pressure in the reactor must be increased as described in Section 3.1.3 for avoiding significant liquid loss due to evaporation during the coating process. Fig. 14a shows schematically the release of molecules from a low vapor pressure liquid that chemically reacts with the PPX precursors. In this way, the nucleation layer will be the product of the reaction and has the potential to functionalize the part of the PPX layer in contact with the liquid. The nucleation layer has the potential to have completely different physico-chemical properties as the PPX. The PPX layer will continue to grow on the nucleation layer as soon as no more molecules are released from the liquid. Such an effect paves the way to user-defined polymer-based electronics as sketched in Fig. 14b where, for example, two different liquids are first deposited by ink-jet printing onto a sacrificial substrate (e.g. glass) leading to two different functionalizations: the yellow liquid becomes a semiconductor due to PPX deposition and reaction, whereas the green liquid ends in a low refraction index layer. Peeling off the PPX layer exhibits the locally defined functionalization. Subsequent metallization (suitable patterning of a sputtered or thermally evaporated metal layer allows contacting the semiconductor, which is in plane with the waveguide. In this way, an extremely thin integrated optics photodiode could be manufactured as a new device based on SOLID technique.

The very first evidence of the creation of such a nucleation layer as chemical reaction between a PPX monomer and a liquid was experimentally brought to evidence by [17]. In this work organic compounds bearing double bond(s) in combination with fluorene fragments were used as substrate. Fig. 10a shows an example where the molecule shown in Fig. 15b (obtained from 9,9-dioctylfluorene-2,7-bis(trimethylborate) and 4-bromostyrene oil), reacts with PPX at nucleation. In total six other molecules have been tested successfully [17].

Further studies have been carried out experimentally and by developing models looking at acrylate structures having a vinyl group polarized by the carboxyl group and the electronegative R_2

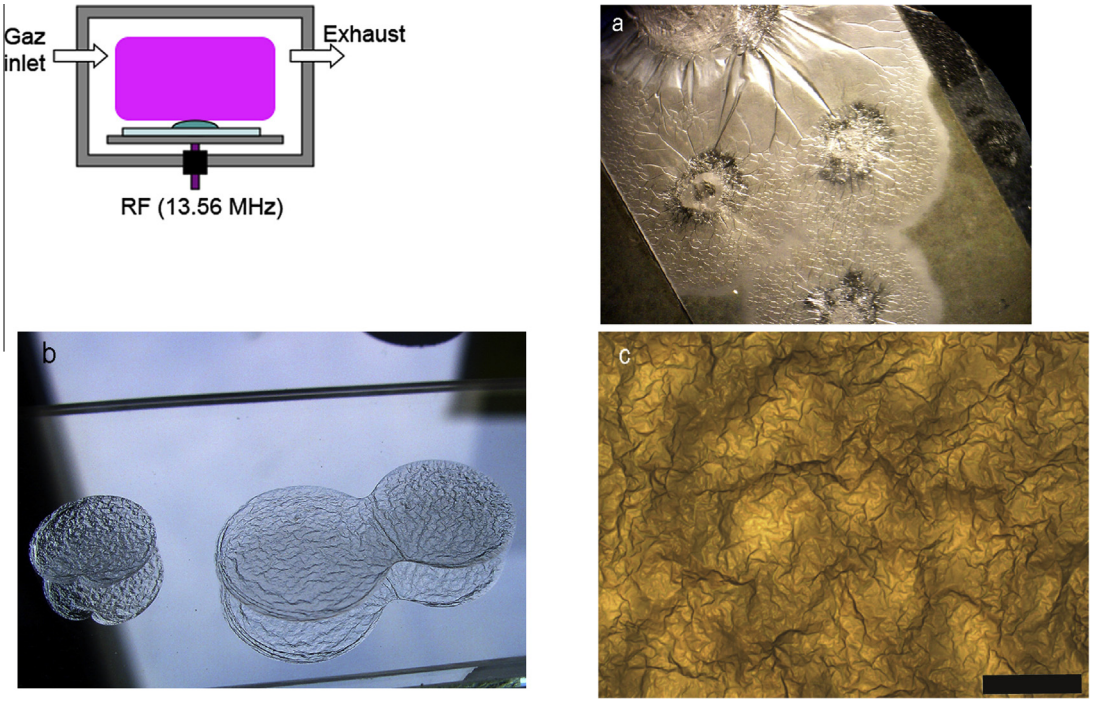

Fig. 10. Sketch of the set-up for deposition using PECVD on silicon oil; (a) a thin film of hydrogenated amorphous carbon layer from C_2H_4 (estimated thickness: 100 nm; width of the substrate 26 mm); (b) SiO_2 layer from HMDS (hexamethyldisilazane) on silicon oil; estimated thickness between 100 and 200 nm; the diameter of the round features varies between 10 mm (left) and 15 mm (middle); the pressure for the PECVD deposition was 5 Pa; the solid surface show pronounced wrinkled due to stress induction from the nucleation of the thin-film; (c) micrograph of the strongly wrinkled hydrogenated amorphous silicon a-Si:H from a 0.5% SiH_4 in Ar PECVD at 5 Pa on silicon oil; the estimated thickness is between 100 and 200 nm; here again, the strong deformation for the originally smooth liquid occurs due to the induced stress at condensation of the layer. The scale bar is 0.5 mm long.

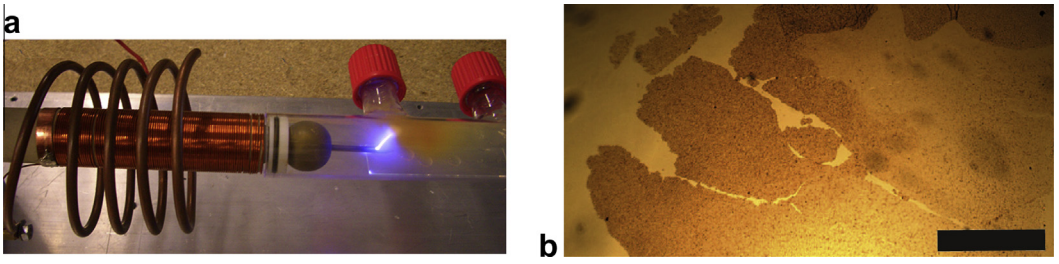

Fig. 11. (a) Set-up with tesla coil for atmospheric corona discharge; (b) deposition of amorphous silicon on silicon oil; no wrinkles are seen here because the surface was very thin (few nm) and not enough molecules could reach the surface to make a continuous layer. The scale bar is 0.5 mm long.

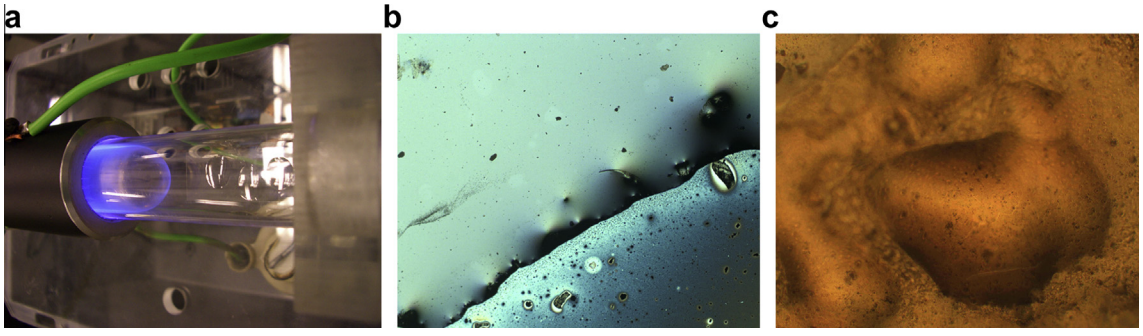

Fig. 12. (a) Silent discharge of a CF_4–Ar plasma, the experiment was carried out at atmospheric pressure; (b) very thin layer of fluor-polymer over silicon oil; estimated thickness below 100 nm at the limit where a continuous solid layer is formed; (c) thicker layer (0.5 μm) of fluor-polymer over silicon oil. Scale given by image width: (b) 200 μm and (c) 3 mm.

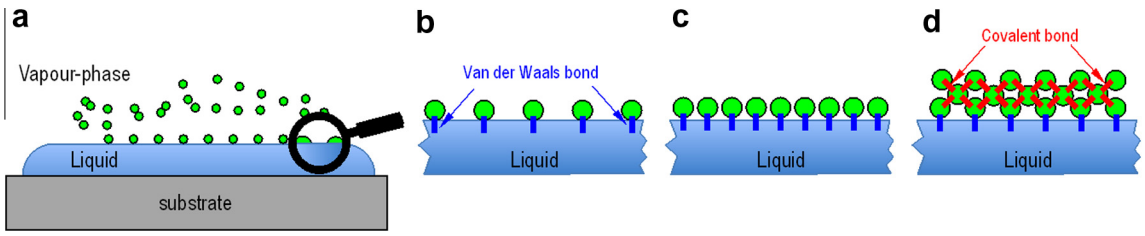

Fig. 13. (a) Particles (molecules, atoms) are first arriving from the vapor phase to the surface of the liquid; the molecules are then weakly bonded at the surface e.g. due to van der Waals bonds; (b) shows a closer look of (a); (c) after some time the density of the particles is increasing, however no cross-linking occurs; (d) after more time, cross linking between the particles occur and a solid-state thin-film is growing; however the internal covalent (or metal bonds) are much stronger, and the initial shape from the surface from the liquid will no longer be able to shape the solid layer from underneath; the residual force vector looking at its minimum energy will finally overtake the shaping of the layer.

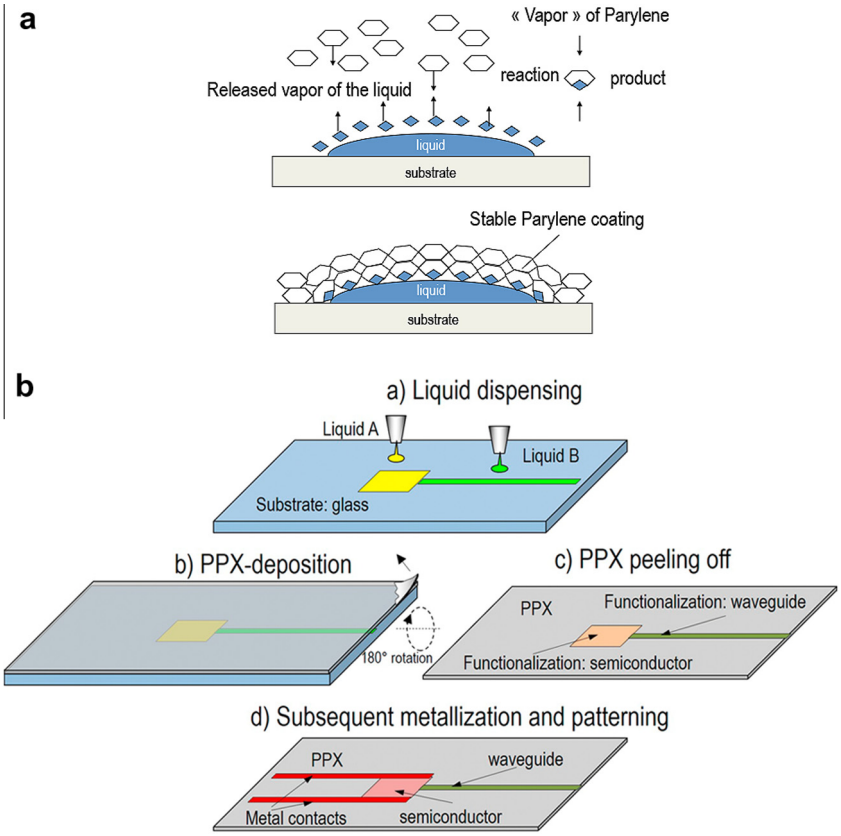

Fig. 14. (a) Creation of a liquid-induced nucleation layer due to a chemical reaction between the PPX precursor and the molecules of the liquid. Peeling off the layer and subsequent cleaning exhibits the functionalization at the place where the liquid has been; (b) vision of a sequence of manufacturing steps for an all polymer electronic system based on two different functionalization of a PPX layer via the choice of the liquid.

substituent. The activation energy for the reaction of the linear biradical paraxylylene dimer DPX with unsaturated $CH_2{=}CR_1{-}COOR_2$ (nucleophile attachment-bond break) was compared with the reaction channel of hydrogen abstraction and conserving the double bond (Pi-bond). Calculations comparing the energies involved in the two reaction channels A and B are shown in Fig. 16 according to [19].

(A). $\cdot DPX\cdot + CH_2{=}CR_1{-}COOR_2 \rightarrow \cdot DPXCH_2C\cdot R_1COOR_2$

(B). $\cdot DPX\cdot + CH_2{=}CR_1{-}COOR_2 \rightarrow \cdot DPXH + HC\cdot{=}CR_1COOR_2 \rightarrow HDPXCH{=}CR_1COOR_2$

Mechanism A was identified as the most promising reaction channel for reaction of PPX-C and acrylate, where radical addition breaks the Pi-bonds. The mechanism is briefly sketched in Fig. 17.

The low value of the activation barrier of about 3 kcal mol^{-1} is comparable to the propagation barriers of polymer chains of parylene. Further reduction of the barrier height can be obtained by modification of the electronegativity via the choice of R_2 as halogenated (X) aromatic rings. The particular low activation energies let one assume that in general unsaturated $CH_2{=}CR{-}$ terminations are potential candidates for further SOLID systems where the nucleations of PPX on the liquid substrate create a functionalized nucleation layer. The kind of functionalization depends on the choice of functional group (R) that is attached to the acrylate group.

Further experiments showed that, indeed, the macroscopic behavior of the PPX layer could be changed. In total, the parylene layers exhibited 14 functionalities [22] such as conductivity, semi conductivity, optical properties etc... For example, we

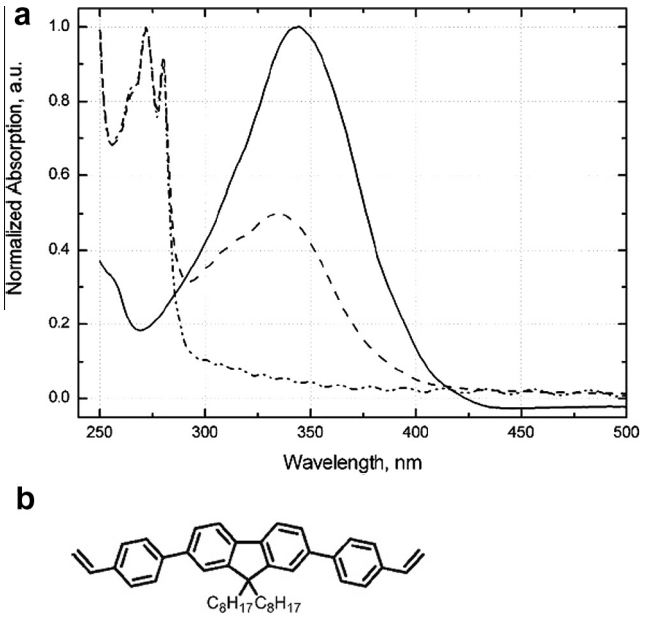

Fig. 15. (a) UV–vis spectra of molecule shown in (b) (solid line), PPX (dash-dotted) and composite from the reaction between the molecules at nucleation of PPX (dashed); special care was taken for subsequent cleaning after the PPX layer after the composite was peeled off (Soxhlet extractor [18]) in order to remove possibly attached residues from the liquid substrate; in the deep UV, the absorption of the composite is dominated by the PPX layer; the peek corresponding to the composite is at 335 nm whereas the peak of the liquid substrate is observed at 343 nm; [[17], permission] (b) the molecule used as liquid substrate is fluorenyldistyrene (2,7-bis-(4-vinylphenyl)-9,9dihexyl-9H-fluorene).

manipulated the conductivity of PPX layers by using sulfonated styrene liquids for the chemical modification of PPX-C surfaces in the course of SOLID process. The polycondensation of 3,4-ethylene-dioxythiophene was then carried out in the presence of modified film (with chemically bonded sulfonic acid groups). The composite obtained demonstrated a surface resistivity of ca. 10^5 Ω measured by a two probe measurement over a 5 mm distance. Note that unreacted PPX-C exhibits a surface resistivity of 10^9 Ω.

4.2. Solid layers on liquid due to plasma induced surface polymerization

In this chapter, the mechanism leading to solid layer creation on a liquid is not due to molecules coming from the vapor phase. Here, the mechanism we are interested in comes from the vapor phase, which is creating itself the cross-linking of the liquids' molecules resulting in a solid layer. This effect depends strongly on the liquid properties, and was observed for polydimethylsiloxane, commonly referred to as PDMS.

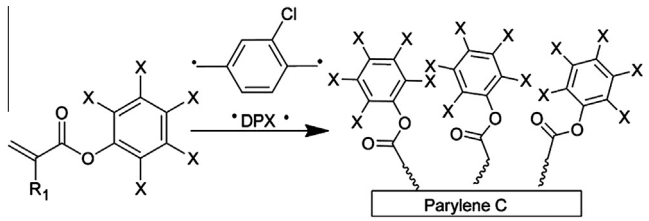

Fig. 17. Radical addition of linear biradical paraxylylene dimer (DPX) on the vinyl carbon leads to consecutive copolymerization because a biradical species is generated as its product, according to [19] permission, [20,21]. The X attached to the aromatic ring stands for halogen.

The usual polymerization of PDMS (Sylgard 184 from Dow Corning) goes like this: a liquid catalyst (part B) is mixed to a precursor (part A) (1:10 mass ratio) in order to induce crosslinking. However, another way to induce this crosslinking was to expose the precursor (part A) to a 3% H_2 in Argon plasma at 13.56 MHz, 20 W power, and a pressure of 50 Pa using a reactor as shown in Fig. 8. This plasma-induced polymerization of the surface is breaking the PDMS precursor into small catalyst molecules with the help of H_2 plasma; this reaction mechanism was proposed by [23]. The atomic hydrogen exposes the liquid surface and leads to cross-linking. The thickness is found to be self-stabilizing, whereby the reaction is first reaction-limited and then diffusion-limited. Subsequent rinsing of the non-cross-linked part A with hexane or ether solvents, allows complete removal of the remaining liquid phase (Fig. 18). With this process, a 200 nm freestanding PDMS layer was obtained [24–25]. Fig. 18a shows a large area petri-dish of the precursor with the layer on it; Fig. 18b shows a freestanding PDMS membrane.

The PDMS solid on liquid must be rather seen as an academic example and not as a direct solution for direct packaging of devices. However it has a high potential as material for manufacturing of hundreds of nanometer thick polymer layers for e.g. sensor applications such as ISFETS membranes [26], and as membranes in the field of biomedical engineering [27–28].

5. Liquid phase methods

In this chapter different techniques are summarized where a "top liquid" is casted on a higher-density "bottom liquid"; both liquids are non miscible. If the top liquid exhibits solidification, a solid on liquid system is obtained.

5.1. Sol–gel method

In this first case, the upper liquid becomes solid due to a sol–gel reaction. As experimental evidence (see Fig. 19), tetraethyl

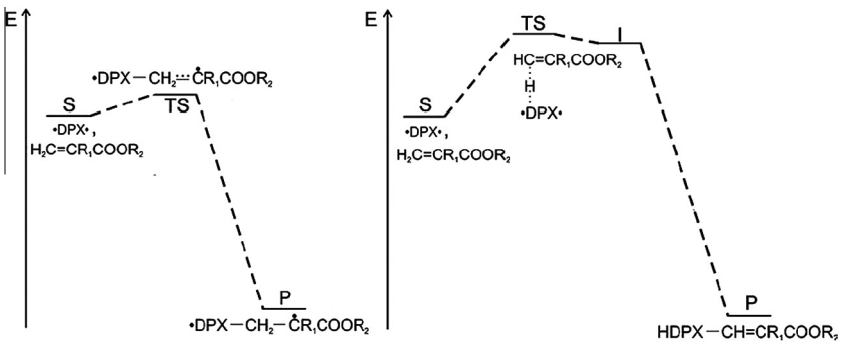

Fig. 16. Energy diagrams for reaction A (left) and B (right). S: substrates, TS: transitions state, I: intermediate product, P: product. E_a is the activation energy from S to TS. It is found that E_a for A is about E_a = 3.2 kcal mol^{-1} and significantly less as compared with B in the E_a = 27.2–28.0 kcal mol^{-1} range [19] permission, [20,21].

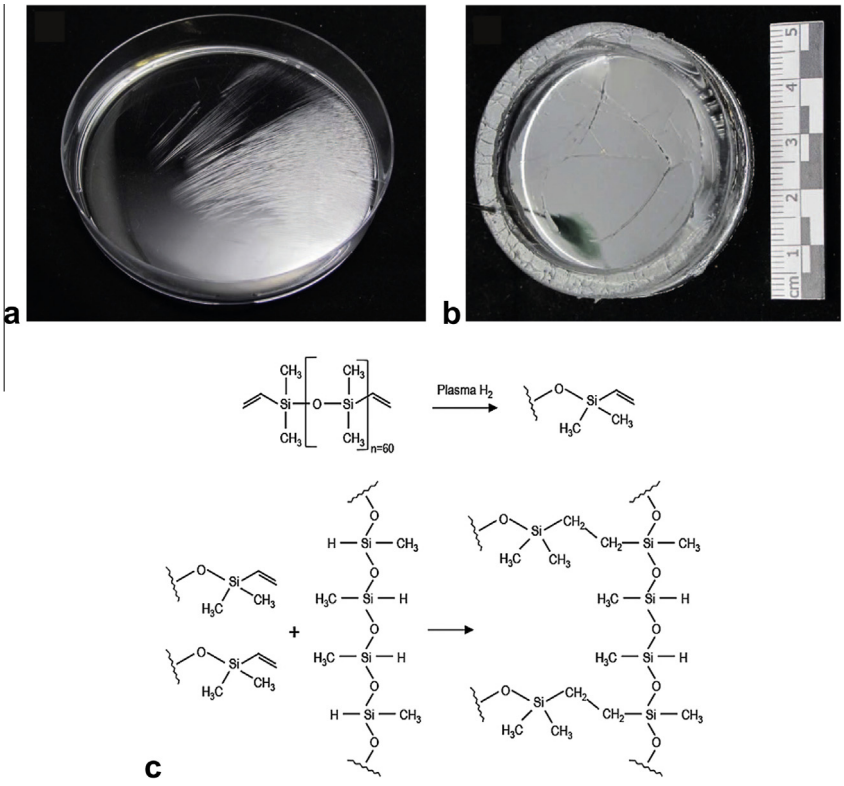

Fig. 18. (a) PDMS part A casted in a plastic petri-dish (85 mm diameter) and treated with 3% H_2 in Argon plasma at 50 Pa, RF plasma at 13.56 MHz, 20 W power, room temperature, and typically 15 min processing time; slight mechanical deformation of the bow let appear wrinkles at the surface that indicate the presence of a closed solid layer on the surface (200 nm thick); (b) freestanding PDMS layer obtained by the procedure described in (a), but with a specially assembled part A container: a polymer ring mounted on a glass plate, according the principle showed in Fig. 6c–e; after casting of part A and subsequent plasma induced polymerization, the bottom plate is sheared off and the non-cross-linked PDMS is rinsed using hexane as a solvent; a large area freestanding PDMS membrane is obtained; (c) reaction mechanism as proposed by [23].

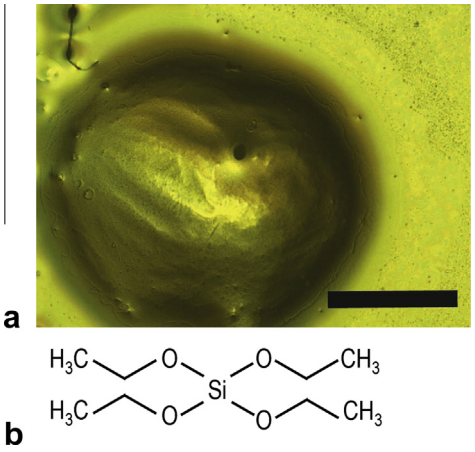

Fig. 19. Solid on liquid deposition by the application of two non-miscible liquids; the top layer (lower density) is tetraethyl orthosilicate TEOS ($Si(C_2H_5O)_4$) that is converted to a stable SiO_2 layer after the evaporation of the solvent (water); the bottom liquid is an ionic liquid 1-butyl-3-methylimidazolium-tetrafluoroborate $[BMIM]^+[BF4]^-$; (b) molecular schematic of the ionic liquid $[BMIM]^+[BF4]^-$. The scale bar is 0.5 mm long.

orthosilicate (TEOS, $Si(C_2H_5O)_4$), with a density of 0.933 g/cm^3, was casted onto an ionic liquid such as $[BMIM]^+[BF4]^-$ (1-butyl-3-methylimidazolium-tetrafluoroborate) that has a higher density (1.21 g/cm^3). After some time TEOS solidifies forming a solid SiO_2 layer on the liquid $[BMIM]^+[BF4]^-$. This SOLID system must be considered as one example among certainly a large variety of similar systems with similar combinations of top and bottom liquids.

In Section 3 we saw that the solid phase is assembled by the accumulation of molecules from the vapor phase onto a liquid phase. The liquid's intermolecular cohesion forces are stronger than gravity and hence density is not an issue. In the case of two non-miscible liquids, the density determines the starting conditions prior to solidification. But apparently, looking at the conversion from BMIM/TEOS to BMIM/SiO_2, the solid SiO_2 layer is not sinking either because the solid is creating one stable solid phase coverage from the beginning, or again because, the cohesion forces at the interface of the bottom liquid prevents from sinking (note the density of SiO_2 is between 2.19 and 2.33 g/cm^3).

5.2. Polymer cross-linking method

In this second example, the upper liquid becomes solid due to a cross-linking reaction. Here the top liquid is a ter-fluoro polymer (tetrafluoroethylene, hexafluoro-propylene, and vinylidene fluoride) called THV-220 [29] (density 1.21 g/cm^3) dissolved in acetone. This acetone-dissolved THV-220 is casted onto glycerol as bottom liquid (density 1.26 g/cm^3). In this case, again, the two liquids are non-miscible and the THV 220 that is completely dissolved in acetone remains as the top liquid. After the evaporation of the acetone, the polymer cross-links (condensation polymerization) and hence coats the glycerol as shown in Fig. 20.

5.3. Sonochemistry-based encapsulation methods

Sonochemistry is a discipline in which chemical reactions are accelerated through the application of ultrasonic sound waves. The physical phenomenon causing sonochemical effects in liquids is acoustic cavitation. It is possible to locally create small centers

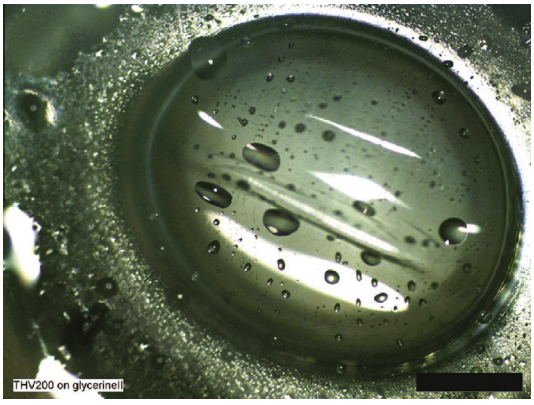

Fig. 20. Solid on liquid deposition obtained by casting in acetone dissolved THV-220 ter-fluoro polymer on glycerol. After evaporation of the acetone, a cross-linked THV-220 coating is obtained. The scale bar is 0.5 mm long.

of high pressure (bubbles) at frequencies of 20 kHz and an ultrasound power of 500 W. The increase of the bubble-size and their subsequent collapse occurs almost adiabatically, where so-called "hot spots" (temperatures between 5000 and 20,000 °C) are created during 1 ns. The surrounding liquid is heated up to 2000 °C. And in the vicinity of those hot spots, pressures between 50 and 150 MPa and extreme cooling rates of 10^{10} K/s are observed [30,31]. "Sonicated" surfaces are exposed hence to conditions whereby activation energies are at hand to undergo chemical processes such as bond breaking but also synthesis. In 1990, water-insoluble liquids could successfully be encapsulated in proteinaceous microcapsules (PM). The effect can be explained in two steps: in a first step emulsification occurs between the non-water-soluble liquid and the protein phase; in the present case the protein BSA (bovine serum albumin) was used. For the second step, the crosslinking (denaturation of proteins) between the protein molecules needs agents such as hydroxyl, superoxide, and peroxide radicals. It was found that, at already 0.3 W, aqueous sonochemistry cause implosive collapses of bubbles that supply the activation energy converting water into hydrogen peroxide [32]. Based on this effect drug delivery systems could be produced by encapsulating tetracycline (TTCL) in a solid protein shell [33]. Solid on liquid deposition is in this case reduced to the solid encapsulation of a liquid in a liquid environment. The encapsulated "containers" have the volume of the emulsified TTCL.

6. Summary and conclusion

In microscale SOLID systems, gravitation effects are negligible as compared to molecular forces. Liquid substrates for thin film deposition from the vapor phase have comparable properties as solid substrates. Based on a large variety of deposition techniques reviewed in this article, we can conclude that solid on liquid deposition is the rule and not the exception.

Along those lines, we showed that any thin film technology and material can potentially be deposited on liquids, however, most of the materials accumulate internal stress leading to the creation of wrinkles and strong deformation due to the low stiffness of liquid surfaces. It seems that parylene is the particular material that does not create internal stress from nanometer to hundreds of micrometer thickness. Therefore, parylene seems to play a particular role.

However, special interest must be paid to the fact that, for a certain choice of liquids, chemical reactions occur at the moment of the nucleation of parylene on the liquid. The agreement between theoretical energy barrier calculations and experiments has confirmed that unsaturated terminated molecules (Pi-bond terminated) together with electronegative substitutes reduce the activation energy needed to add biradical PPX. This effect has the potential of creating a large variety of functionalization and manufacturing of all polymer-based electronic devices.

Bubble-free and stress free coating on varying liquid geometries based on solid on liquid technology can enable devices such as micro lenses and liquid waveguides. Removing the liquid creates volumes or channels for fluidic systems, free standing membranes, and 3D MEMS.

Acknowledgements

This work was supported by the EU projects MULTIPOL (under contract FP6-NMP3-CT-2006-033201), PARYLENS (under contract FP7-NMP-2009-246362), and NANOCI (under contract FP7-NMP.2011–281056). This work was also supported by a CTI-Discovery project Grant Nr. 8241.1 DCS-NM, and by the HES-SO// University of Applied Sciences Western Switzerland (projet Muchsens, programme thématique I1 Diagnostic biochips).

Thanks also to Prof. Sumita Pennathur and to both reviewers of this paper for their contribution to improving the clarity of this paper.

References

[1] H. Keppner, M. Benkhaïra, Method for producing a plastic membrane device and the thus obtained device, Patent WO/2006/063955, 2004.
[2] J. Charmet, O. Banakh, E. Laux, B. Graf, F. Dias, A. Dunand, H. Keppner, G. Gorodyska, M. Textor, W. Noell, N.F. de Rooij, A. Neels, M. Dadras, A. Dommann, H. Knapp, Ch. Borter, M. Benkhaira, Solid on liquid déposition, Thin Solid Films 518 (2010) 5061–5065 (Permission: company number 1982084; Licence Number: 3501461236946 reprinted Figs. From Elsevier Thin solid films; Fig. 5a, 5 b, 7; used in this paper Fig. 5a, 5b, 5c).
[3] B.K. Nguyen, E. Iwase, K. Matsumoto, I. Shimoyama, MEMS 2007, Kobe, Japan, 2007, pp. 305–308 (Permission: License number: 3501471104051 date: 03.11.14; reprinted figure from IEEE MEMS 2007, Fig. 6; used in this paper: Fig. 4b).
[4] W.F. Gorham, A. New, J. Polym. Sci. A Polym. Chem. 4 (1966) 3027–3039.
[5] J.B. Fortlin, T.M. Lu, Chemical Vapour Deposition Polymerization the Growth of Parylene Thin Films; Kluwer Academic Publishers Boston, Dordrecht/New York/London. ISBN 1 4020 7688 6.
[6] K. Smalara, A. Gieldon, M. Bobrowski, J. Rybicki, C. Czaplewski, J. Phys. Chem. A 114 (12) (2010) 4296–4303.
[7] D.W. Grattan, Can. Chem. News (1989) 25–26.
[8] N. Binh-Khiem, K. Matsumoto, I. Shimoyama, MEMS 2011, Cancun, MEXICO 2011 (2011) 111–114.
[9] D. Falconnet, A. Koenig, F. Assi, Adv. Funct. Mater. 14 (8) (2004) 749–756.
[10] H.J. Whitlow, R. Norarat, M. Roccio, P. Jeanneret, E. Guibert, M. Bergamin, G. Fiorucci, A. Homsy, E. Laux, H. Keppner, P. Senn, Nucl. Instr. Meth. B (in press), doi: 10.1016/j.nimb.2014.10.024.
[11] J. Brossard, A. Homsy, M. Roccio, P. Senn, H. Keppner, Multilayer Laser Patterning of Parylene, EPFL – MicroNanoFabrication Annual Review Meeting, Lausanne, Switzerland, 2014.
[12] <www.comelec.ch/en/parylene_tableaux.php> (webpage accessed on 23.02.15).
[13] S. Uhl, E. Laux, T. Journot, L. Jeandupeux, J. Charmet, H. Keppner, Proc. of 11. ECT 2013 Conference Noordwijk Springer. ISBN: 978-3-319-07331-6 (print) 978-3-319-07332-3 (online).
[14] D. Wileńska, I. Anusiewicz, S. Freza, M. Bobrowski, E. Laux, S. Uhl, H. Keppner, P. Skurski, Mol. Phys. (submitted for publication).
[15] R. Clausius, Ann. Phys. 155 (4) (1850) 500–524.
[16] M.C. Clapeyron, J. Polytech. 23 (1834) 153–190.
[17] A. Bolognesi, C. Botta, A. Andicsova, U. Giovanella, S. Arnautov, J. Charmet, E. Laux, H. Keppner, Macromol. Chem. Phys. 210 (2009) 2052–2057, http://dx.doi.org/10.1002/macp.200900321 (Permission: License number: 3501491304842 date: 03.11.14; reprinted figure from John Wiley & sons, Macromol. Chem. Phys.).
[18] L.M. Harwood, C.J. Moody, Experimental Organic Chemistry: Principles and Practice (Illustrated ed.), Wiley-Blackwell (13.06.89), pp. 122–125. ISBN: 0-632-02017-2.
[19] M. Naddaka, F. Asen, S. Freza, M. Bobrowski, P. Skurski, E. Laux, J. Charmet, H. Keppner, M. Bauer, J.-P. Lellouche, Polym. Chem. (2011), http://dx.doi.org/10.1002/POLA24731 (Permission: License number: 3501500055201 date: 03.11.14; reprinted figure from John Wiley & sons, J. Polym. Sci. A Scheme 1 and Fig. 1; used in this paper: Figs. 12, 11).
[20] K. Smalara, A. Gieldon, M. Bobrowski, J. Rybicki, C. Czaplewski, J. Phys. Chem. A 114 (2010) 4296–4303.

[21] S. Freza, P. Skurski, M. Bobrowski, Chem. Phys. 368 (2010) 126–132 <www.elsevier.com/locate/chemphys>.
[22] MULTIPOL (European project FP6) – NMP3-CT-2006-033201, Deliverable 16, 2010.
[23] A. Thangawng, R. Ruoff, M. Swartz, M. Glucksberg, Biomed. Microdev. 2007 (9) 587–595.
[24] E. Laux, J. Charmet, H. Haquette, O. Banakh, L. Jeandupeux, B. Graf, H. Keppner, Processes in Isotopes and Molecules, IOP Publishing 182 (2009) 012029, http://dx.doi.org/10.1088/1742-6596/182/1/012029.
[25] Y. Rebetez, Réalisation de membranes ultraminces en PDMS (Bachelor's thesis), Haute Ecole Arc Ingénierie, HES-SO//University of Applied Sciences Western Switzerland, 2013.
[26] J.C. Löttersy, W. Olthuis, P.H. Veltink, P. Bergveld, J. Micromech. Microeng. 7 (1997) 145–147.
[27] B Balakrisnan, S Patil, E Smela, J. Micromech. Microeng., doi:10.1088/0960-1317/19/4/047002.
[28] A.L. Thangawng, R.S. Ruoff, M.A. Swartz, R. Matthew, Glucksberg, Biomed. Microdev. 9 (2007) 587–595, http://dx.doi.org/10.1007/s10544-007-9070-6.
[29] H. Teng, Appl. Sci. 2 (2012) 496–512, http://dx.doi.org/10.3390/app2020496.
[30] K.S. Suslick, The Chemical Effects of Ultrasound, Scientific American, 1989, pp. 62–68.
[31] K.S. Suslick, M.W. Grinstaff, J. Am. Chem. Soc. 112 (1990) 7807.
[32] T.Y. Wu, N. Guo, C.Y. Teh, J.X.W. Hay, Advances in Ultrasound Technology for Environmental Remediation, Springer, 2013. ISBN: 978 94 007 5532 1.
[33] S. Avivi, Y. Nitzan, R. Dror, A. Gedanken, J. Am. Chem. Soc. 125 (2003) 15712–15713.